1-1-2015

Characterisation of torsional actuation in highly twisted yarns and fibres

Shazed Aziz
University of Wollongong, sma280@uowmail.edu.au

Sina Naficy
University of Wollongong, snaficy@uow.edu.au

Javad Foroughi
University of Wollongong, foroughi@uow.edu.au

Hugh Ralph Brown
University of Wollongong, hbrown@uow.edu.au

Geoffrey M. Spinks
University of Wollongong, gspinks@uow.edu.au

Characterisation of torsional actuation in highly twisted yarns and fibres

Abstract

Highly twisted oriented polymer fibres and carbon nanotube yarns show large scale torsional actuation from volume expansion that can be induced, for example, thermally or by electrochemical charging. When formed into spring-like coils, the torsional actuation within the fibre or yarn generates powerful tensile actuation per muscle weight. For further development of these coil actuators and for the practical application of torsional actuators, it is important to standardise methods for characterising both the torsional stroke (rotation) and torque generated. By analogy with tensile actuators, we here introduce a method to measure both the free stroke and blocked torque in a one-end-tethered fibre. In addition, the torsional actuation can be measured when operating against an externally applied torque (isotonic) and actuation against a return spring fibre (variable torque). A theoretical treatment of torsional actuation was formulated using torsion mechanics and evaluated using a commercially available highly-oriented polyamide fibre. Good agreement between experimental measurements and calculated values was obtained. The analysis allows the prediction of torsional stroke under any external loading condition based on the fundamental characteristics of the actuator: free stroke and stiffness.

Keywords

characterisation, torsional, fibres, actuation, yarns, highly, twisted

Disciplines

Engineering | Physical Sciences and Mathematics

Publication Details

Aziz, S., Naficy, S., Foroughi, J., Brown, H. R. & Spinks, G. M. (2015). Characterisation of torsional actuation in highly twisted yarns and fibres. Polymer Testing, 46 88-97.

Characterisation of torsional actuation in highly twisted yarns and fibres

Shazed Aziz[a], Sina Naficy[a,b], Javad Foroughi[a], Hugh R. Brown[a] and Geoffrey M. Spinks[a,b]*

[a] *ARC Centre of Excellence for Electromaterials Science and Intelligent Polymer Research Institute, University of Wollongong, Innovation Campus, Squires Way, North Wollongong, NSW, 2522, Australia.*

[b] *School of Mechanical, Materials and Mechatronic Engineering, University of Wollongong, Wollongong, NSW, 2522, Australia.*

**to whom all the correspondence should be addressed*

Tel +61 2 4220 3010; gspinks@uow.edu.au

Abstract

Highly twisted oriented polymer fibres and carbon nanotube yarns show large scale torsional actuation from volume expansion that can be induced, for example, thermally or by electrochemical charging. When formed into spring-like coils, the torsional actuation within the fibre or yarn generates powerful tensile actuation per muscle weight. For further development of these coil actuators and for the practical application of torsional actuators, it is important to standardise methods for characterising both the torsional stroke (rotation) and torque generated. By analogy with tensile actuators, we here introduce a method to measure both the free stroke and blocked torque in a one-end-tethered fibre. In addition, the torsional actuation can be measured when operating against an externally applied torque (isotonic) and actuation against a return spring fibre (variable torque). A theoretical treatment of torsional actuation was formulated using torsion mechanics and evaluated using a commercially available highly-oriented polyamide fibre. Good agreement between experimental measurements and calculated values was obtained. The analysis allows the prediction of torsional stroke under any external loading condition based on the fundamental characteristics of the actuator: free stroke and stiffness.

1. Introduction

Giant torsional actuation from highly twisted fibres and yarns has been recently discovered [1-6] with potential applications in microfluidic mixing [1] and digital displays [3]. Volume expansion induced thermally, chemically, photonically or electrochemically causes partial untwist of highly twisted carbon nanotube, graphene or oriented polymer fibres and yarns [1, 6]. Rotations per actuator length of such twisted structures were 1000 times larger than previously reported systems [7, 8]. Additionally, it was discovered that when the torsionally-actuating fibres and yarns are converted to coils, for example by extreme twist insertion, the fibre untwist translates to expansion or contraction along the coil axis. Tensile strokes as high as 49% were reported for twisted and coiled nylon-6,6 fibres delivering 2.48 $kJ.kg^{-1}$ contractile work capacity [6] and greatly exceeding that generated by natural skeletal muscle (39 $J.kg^{-1}$) [9, 10].

To aid material development for torsional muscle, the present work aims to develop a test method for assessing torsional actuation. Of interest is a procedure to characterize torsional stroke and torque as well as an assessment of speed, reversibility and cycle life. Previous work has focussed mainly on measuring torsional stroke, for example by tethering the sample at one end and measuring the rotation of the free end. Sometimes a return spring mechanism has been used to improve reversibility of torsional actuation. In these cases, the actuating yarn or fibre was attached to another non-actuating fibre, both ends were tethered and torsional rotation measured at the junction. An advantage of the two-end-tethered system is the ability to fix the location of the rotating element. In contrast, the free end of the one-end-tethered system can move in any direction and has limited practical utility.

What is needed is a measurement technique and analysis procedure that allows the torsional stroke and torque to be calculated for any imposed external loads. By analogy with tensile actuators, the characterisation method should provide the stroke-torque curve defining the free stroke (zero external torque), blocked torque (zero torsional rotation) and all combinations of non-zero stroke and torque. Such information has not yet been reported for any of the twisted fibre torsional muscles. Herein is described a method for measuring the rotation of a shaft attached to a near frictionless bearing and driven by a torsional actuator, *i.e.* the twisted fibre. The measurement system can measure both torsional stroke and torque, and the sample can either be operated with or without a return spring fibre.

The theoretical treatment of torsional actuation assumes that a given stimulus induces a free rotation that increases linearly with fibre length, and is here denoted θ and reported as degrees per mm of actuating fibre length. The actual rotation angle $\phi(x)$ varies linearly with distance x taken from the clamped end of a fibre so that the torsional stroke at the free end of a one-end-tethered fibre of length L_A is:

$$\phi(L_A)_{free} = L_A.\theta \tag{1}$$

If the fibre behaves as a linear elastic rod in torsion, then the blocked torque will be:

$$\tau_{blocked} = \phi(L_A)_{free} \times S_A \quad (2)$$

Here, S_A is the torsional rigidity of the actuating fibre, or the resistance to rotation. The torsional stiffness is more fundamentally related to the fibre diameter (d), length (L) and the fibre material's shear modulus (G) in the circumferential direction:

$$S = \frac{k}{L} = \frac{JG}{L} \quad (3)$$

where, k is termed the 'torsional modulus' in standard torsion mechanics and should not be confused with other moduli, such as the shear modulus and Young's modulus that are true material properties. The torsional modulus depends both on material properties and the fibre dimensions. J is the polar moment of inertia of the fibre and formulated in terms of sample diameter for a fibre of circular cross-section is:

$$J = \frac{\pi d^4}{32} \quad (4)$$

The stimulus used to initiate torsional actuation, for example heat, is likely to affect the material's torsional stiffness due to dimensional changes and modulus shift. Consequently, the blocked torque represented by equation (2) uses the torsional stiffness of the fibre in the final actuated state after the stimulus has been applied (hereafter denoted S'_A). A change in torsional stiffness will also contribute to the torsional stroke measured under isotonic (constant external torque) conditions. For a one-end-tethered fibre acting against an external torque τ_{ext} the torsional stroke will be given by:

$$\phi(L_A)_{isotonic} = L_A\theta + \tau_{ext}\left(\frac{1}{S'_A} - \frac{1}{S_A}\right) \quad (5)$$

The second term in equation (5) relates to the free end rotation resulting from a change in sample torsional stiffness from S_A to S'_A in the starting and final states, respectively.

When operated against a return spring, the external torque acting against the actuating fibre increases after the stimulus has been applied. The return spring is twisted as the actuating fibre torsionally actuates generating a restoring torque within the return spring fibre. The rotation at the end of the actuating fibre, corresponding to the junction between the actuating and non-actuating fibres, will be smaller than in free rotation so a residual torque remains in the actuating fibre. At equilibrium, the residual torque in the actuating fibre is exactly cancelled by the restoring torque generated in the return spring, non-actuating fibre. For the general case where the actuating fibre is subjected to a constant external torque and connected to a return spring fibre of torsional stiffness S_N, the torsional stroke (ϕ) at the junction between actuating and non-actuating fibres can be determined from the torque balance equation:

$$S'_A\left[\left\{L_A\theta + \tau_{ext}\left(\frac{1}{S'_A} - \frac{1}{S_A}\right)\right\} - \phi\right] = S_N\phi \quad (6)$$

Re-arranging equation (6) gives an expression for the expected torsional stroke at the junction between the actuating and non-actuating fibres:

$$\phi(L_A)_{return\ spring} = \left[L_A\theta + \tau_{ext}\left(\frac{1}{S'_A} - \frac{1}{S_A}\right)\right]\left(\frac{S'_A}{S'_A+S_N}\right) \quad (7)$$

In the case where the external torque is zero, the stroke is given by:

$$\phi(L_A)_{return\ spring} = L_A\theta\left(\frac{S'_A}{S'_A+S_N}\right) \quad (8)$$

Equation (8) reduces to equation (1) in the absence of a return spring (S_N=0) and when the actuating fibre is tethered at only one end. Figure 1 illustrates the theoretical torsional stroke expected for the case of free rotation, isotonic torsional actuation and torsional actuation with a return spring. The torsional strokes are expressed as a fraction of the free rotation to emphasise the importance of the inherent torsional actuation parameter, θ, in determining the torsional stroke in all cases.

2. Experimental methods

2.1 Muscle fabrication

Twist insertion into commercially available nylon 6 fibre (~550 µm diameter Sport Fisher monofilament fishing line) was conducted by an electrical DC motor. The fibre was attached to the motor at its upper end and supported by a fixed weight (~200 gm) hanging on the other end providing 10 MPa stress to the fibre. The incorporated weight was tethered contrary to the motor rotation, and hence each turn from the motor shaft caused the formation of one turn in the fibre. The muscle fibre taken for the actuation test was twisted until the onset of coiling. The supported weight on the fibre was crucial to have straight and uniformly twisted fibres, without permitting snarl formation prior to coiling. The non-coiled section of twisted fibre was then taken to an isothermal heating oven and annealed at 120°C, or ~70^{o}C above glass transition (T_g) [11, 12], for 30 minutes with both ends clamped to prevent loss of twist. Heating at a temperature over T_g helps the newly introduced twisted shape to be permanently set. After removal from the oven, the fibre was relaxed at room temperature for 2 hours while still clamped. Figure 2 shows a schematic diagram of twist insertion and the preparation of fishing line muscle to be used for actuation tests.

Twist insertion per length of precursor fibre was determined by using a rotation counter. Fibre bias angle (α_f, relative to fibre axis) due to the twist insertion was calculated from the number of turns/meter using Equation (9) [1].

$$\alpha_f = tan^{-1}(\pi dT) \quad (9)$$

Here, *d* is the fibre diameter and *T* is the amount of turns inserted per initial fibre length.

Additionally, the fibre bias angle was observed directly using an optical microscope (LEICA M205 A). The observed bias angle was in close agreement with the value calculated using equation (9) from the measured number of turns/meter inserted into the twisted fibre.

2.2 Thermally-powered torsional actuation test

Experiments were conducted using an in-house-produced torsional actuation test apparatus with a heating chamber (Figure 3). The heating process was operated through Nichrome 80/20 heating wire and driven by an electrical current source. Twisted nylon fibre was positioned in the heating zone to evaluate the torsional actuation performance during heating and cooling cycles. A thermocouple was positioned close to the sample to estimate sample temperature.

A slow heating process (3.5°C/min) was maintained by using a programmable controller (Electro Chemical Engineering Pty Ltd, Australia) to increase temperature at a uniform rate from 25°C to 60°C. Figure 4 shows the integrated experimental set-up consisting of test apparatus, programmable power supply and dual-mode lever arm system (Aurora Scientific, Canada). In all cases, it was found that a small number of heating and cooling cycles were needed before the torsional actuation became fully reversible. Data measurements were conducted after the completion of these 'training cycles'. Samples were equilibrated in ambient laboratory conditions before testing and separate studies between carefully dried and water-saturated samples showed negligible difference in actuation behaviour.

Initial interest was to quantify the amount of torsional stroke generated by the twisted fibre in a certain range of temperature. The fibre was tethered to a rigid support at one end and the other end was clamped to an aluminium shaft (radius, r_s) passing through a pair of aligned air bearings (OAVRL13MM supplied by CGB Precision Products Pty Ltd, USA) mounted on aluminium supports. These compressed air assisted bearings are able to provide almost frictionless rotation, so that torsional motion can freely occur with negligible external disturbance to the actuated fibre. The amount of thermally powered free torsional stroke generated by the twisted fishing line was observed optically by using a microscopic camera system (ISSCO-OPTEK). The camera was positioned and focused axially to the air bearing and videography of bearing rotation was exported to a geometric tool (GeoGebra mathematics software) to quantify the amount of fibre rotation.

The optical method for determining torsional stroke could not provide real-time data, so the test apparatus was modified by introducing a dual-mode lever arm force/distance transducer (Aurora 305B). The air bearing shaft was partially wrapped with a high stiffness thin polyethylene fibre (DYNEEMA 180 μm diameter) and connected to the lever arm operated in isotonic mode (constant force) and positioned so that the connecting fibre was perpendicular to the shaft. Torsional actuation of the twisted fibre rotated the connecting shaft which caused proportional displacement of the lever arm that was then

expressed as the torsional stroke (degree). Calibration of lever arm displacement to shaft rotation was performed in terms of shaft circumference and angular movement that caused the linear motion of vertically placed lever arm. The lever arm applied a small and constant normal force (F_N) to the shaft resulting in a constant torque ($\tau_S=F_N.r_s$). Unless otherwise stated, the external force opposed the rotation of the twisted fibre when the latter was heated.

The same apparatus was also used to evaluate the torque generated during heating/cooling of the twisted nylon fibre. In this case the lever arm was operated in the isometric mode (constant length) to prevent shaft rotation and provide a measure of the blocked torque. Torque/stroke curves could also be obtained by first measuring the blocked torque and then allowing the shaft to rotate by gradually reducing the applied force to zero while measuring the amount of shaft rotation.

Of further interest was to assess the amount of torsion when the actuating fibre was attached to a 'return spring', as has been typically used in previous studies. As shown in Figure 2, a return spring fibre can be included by attachment to the air bearing shaft and a second end tethering point. Tension is sometimes also applied using the return spring fibre.

2.3 Fibre characterization

The torsional rigidity (S) [13], torsional modulus ($k=JG$) [1] and shear modulus (G) [14] of both the twisted (actuated) fibre and return spring fibre were determined by measuring the shaft rotation resulting from mechanical increase of torque applied by the lever arm. Torsional rotation (ϕ) versus torque (τ) curves from multiple samples of different lengths was used to determine torsional rigidity of fibre, as in equation (2).

3. Results

3.1 Characteristic properties of twisted fibre

A nylon 6 fibre of 550 µm diameter (d) was used for twist insertion. Figure 5 shows optical micrographs at different stages of the twisting process. Figure 5(a) represents the precursor fibre and Figures 5(b) and (c) show, respectively, the coiled and non-coiled portions of fibre after insertion of 450±5 turns per metre of initial fibre length. The highly twisted, but non-coiled section of muscle fibre was extracted for further analysis. Fibre diameter was found to have increased during twisting by ~10% from ~551 µm to ~597 µm. The bias angle of inserted twist was calculated from Equation (9) and found to be 35.3°. Figure 4(d) shows optical measurements of the fibre bias angle showing 36.0° from the fibre axis, which is in close agreement with the calculated value.

The torsional stiffness and moduli of the twisted nylon 6 fibres were evaluated from inverse gradient of stroke/torque plots (Equation 2) and gradient of corresponding

stiffness/inverse length plot (Equation 3). Figure 6(a) shows that shaft rotation linearly progresses as the amount of mechanically applied torque increases. Three different sample lengths (10, 35, and 70 mm) of identical twisted fibre were considered and showed a linear relationship between torsional stiffness and length (Figure 6(b)). The resulting length independent torsional modulus was found to be 3.56×10^{-6} N.m^2 at room temperature.

Torsional properties of nylon 6 fibre were also evaluated in terms of fibre diameter. Figure 7(a) shows the angular rotation of two fibres under increasing external torque: a twisted nylon 6 fibre of original length of 10 mm long and 550 μm diameter (d_2) and an untwisted fishing line 10 mm long and 330 μm diameter (d_1) that was used as a return spring in some actuation experiments. The torsional moduli were 3.56×10^{-6} N.m^2 for the twisted fibre and 4.7×10^{-7} N.m^2 for the return spring.

$$\frac{k_1}{k_2} = \left(\frac{d_1}{d_2}\right)^4 \tag{10}$$

Here, k_1 and k_2 are the torsional moduli of the twisted fibre and the return spring fibre, respectively. Experimental results (Figure 7(b)) show the torsional modulus ratio to be 7.57, in reasonable agreement with the fourth power of the diameter ratio (7.72), as predicted by theory. The shear moduli of twisted nylon 6 fibre and untwisted return spring were very similar (0.40 GPa and 0.41 GPa, respectively) as is expected for fibres with the same composition and structure.

Torsional properties of the 550 μm twisted fibre were also evaluated at the maximum temperature reported for actuation tests in this study. Figure 8 shows the angular movement of twisted fibres at 60ºC under increasing external torque. The torsional modulus was 3.19×10^{-6} N.m^2. Shear modulus of the twisted fibre at this particular temperature were calculated by considering the change in fibre diameter resulted from applied heat and found to be ~0.24 GPa, which is significantly lower than the value obtained at room temperature, as expected [15].

3.2 Torsional actuation test results

3.2.1 Free fibre rotation

In free rotation tests, the twisted nylon 6 fibre was attached at one end to the air bearing shaft and the other end clamped. Heating allowed the non-clamped fibre end to rotate freely with negligible external resistance. Figure 9 shows optically measured torsional rotation of the air bearings. The fibre was observed to rotate in the untwist direction during heating and to retwist on cooling in the range 28-62ºC. The rate of rotation was higher above ~50ºC, which corresponds approximately to the T_g of nylon 6. A small hysteresis between heating and cooling was observed, especially above T_g. The final rotation angle after heating to 62ºC reached an approximately constant value of -171º, or -2.45º/mm based on fibre length, after several heating and cooling cycles.

3.2.2 Constant torque torsional actuation

The torsional actuation of the twisted fibre was also tested isotonically under constant torque. Figure 10 shows the thermally driven torsional stroke of twisted fibre acting against a constant torque in the up-twist direction of ~68 µN.m applied to the bearing shaft surface when the sample was subjected to heat/cool cycles in the range of 28-62ºC. The torsional stroke was calculated from the lever arm deflection and was validated by optical measurements of the bearing rotation that demonstrated 99.5% accuracy. Hence, it was concluded that the lever arm provides immediate, convenient and continuous measurement of the fibre rotation without the need for off-line image analysis.

The thermally-induced isotonic torsional stroke of the nylon 6 was similar to that observed during free rotation. The 70 mm long and 550 µm diameter twisted nylon 6 generated a maximum -2.32°/mm fully reversible torsional rotation when heated slowly from 28 ºC to 62 ºC (Figure 10). The maximum rotation angle from cycle to cycle was more consistent than in free rotation tests. The original shape was regained after the cooling cycle by retwisting the fibre with almost 100% reversibility. The complete re-twist on cooling was assisted by the small torque applied by the lever arm. Again, a higher rate of rotation was observed above T_g of ~50ºC. A small hysteresis between heating and cooling cycles of unknown origin occurred at lower temperatures between 30-40ºC.

Similar tests were also conducted using several different constant applied torque values. In all cases, the torque was applied so as to oppose the fibre untwisting that occurred during heating. Figure 11 shows the torsional stroke during heating and cooling with increase of torque occurring in successive actuation cycles. The torque adjustment occurred isothermally at 26ºC and torsional stroke in each actuation cycle is reported after training the sample by several heating/cooling cycles at each new torque level. As shown, the actuation stroke after heating from 26-62ºC decreased as the opposing torque increased. The torque was increased by a factor of ~16 times resulting in a decrease in the torsional stroke of ~32%. A final heat/cool cycle was performed after resetting the torque to its initial value, and the results show that the torsional stroke followed the original curve very closely. It can be concluded that the higher torque isotonic tests caused no degradation or other permanent effects on the torsional actuation behaviour of the twisted nylon 6 fibre.

3.2.3 Torque generation and torque-stroke curves

The torque generated during heating and cooling of the twisted fibres was determined by isometric testing where the fibre rotation was completely blocked by the lever arm and the blocking force measured. The samples were first conditioned using the normal training cycles where the fibre was allowed to freely rotate until the untwist and retwist on heating and cooling became fully reversible. At this point, the blocked rotation test was performed and a 70 mm long and 550 µm diameter twisted fibre was able to produce ~225 µN.m torque when the sample was heated from 28 to 62ºC (Figure 12). On cooling, the torque

returned to the starting value, demonstrating the reversibility of the torsional actuation. A noteworthy hysteresis was observed between the torque generated in the heating and cooling cycles. The hysteresis was mostly due to a small force decay that occurred during the isothermal hold period at the maximum temperature and prior to cooling.

Torque-stroke curves were also generated by first measuring the blocked force during heating and then allowing the fibre to untwist isothermally until the torque was fully relaxed. The fibre was next retwisted isothermally to restore the measured blocked force and the sample cooled under isometric conditions. Figure 13(a) shows the testing sequence and Figure 13(b) shows the torque-stroke curves obtained during the isothermal period at 60ºC. The fibre was allowed to untwist as the torque was relaxed and the free rotation stroke could be estimated from the zero torque point on the curve. Here, the free torsional stroke was -204º or -2.91º/mm (Figure 13(b)). Interestingly, this free stroke value was significantly higher than measured during the free rotation experiments (-2.45 º/mm). The slope of the torque-stroke curve also provides a measure of the fibre torsional modulus at 60ºC giving a value of 4.26×10^{-6} N.m^2 for the 70 mm long twisted fibre. Again, this value is higher than the torsional modulus reported above. Possible explanations for these differences are considered in the Discussion section.

3.2.4 Variable torque torsional actuation using a return spring

This experiment was conducted by thermally actuating the twisted fibre against a return spring, as has been commonly used in previous studies [1]. The test system included a second nylon 6 fibre connected to the opposite end of the air bearing shaft and then tethered to the supporting frame. Here, rotation of the shaft resulted from torsional actuation of the actuating fibre twists the return spring fibre, thereby generating an increasing opposing torque as the sample rotation proceeds. In addition to the return spring torque, the lever arm was operated in isotonic mode and applied a small constant torque of 68 µN.m that also opposed the sample rotation. This small torque was necessary for accurate measurement of the shaft rotation using the lever arm displacement transducer. Figure 14 shows the thermally induced torsional stroke of a 70 mm long, 550 µm diameter twisted nylon 6 fibre acting against the variable torque applied by a 70 mm long and 330 µm diameter nylon 6 return spring. Fully reversible torsional actuation was observed during heating and cooling in the range of 28-62ºC with very little hysteresis. The maximum rotation angle decreased slightly during successive cycles to a value of -2.04º/mm, which was considerably smaller than rotations observed in free rotation tests due to the restrictions imposed by the return spring. The quantitative evaluation of the return spring effects is considered in Section 4.

The effect of spring stiffness on torsional stroke was also investigated by using different lengths of return spring fibres. Starting from 70 mm, the spring length was decreased by

~14 times in five stages (Figure 15). The corresponding torsional stroke of the same actuating fibre was decreased by ~61% when comparing the shortest return spring with the longest return spring fibre and using a constant 26-62ºC temperature range. A final heat/cool cycle was performed using the initial spring length and the actuation behaviour was almost identical to the first heat/cool cycle.

4. Discussion

The main aim of the present work was to establish a method for analysing torsional actuation obtained from different test methods. The analysis starts with the 'free' torsional stroke per fibre length of θ (deg/mm) obtained experimentally from actuating fibres tethered at only one end[1]. The effect of a return spring and/or an externally applied torque on the torsional stroke is theoretically shown in equation (7). Finally, the expected torque generated is given by the product of torsional stroke and final torsional stiffness with the maximum torque predicted from equation 2 (blocked torque). These analyses suggest that all torsional actuation parameters can be determined from knowledge of the free stroke (θ), actuating fibre stiffnesses (S_A and S'_A for initial and final temperatures, respectively), return spring stiffness (S_N) and actuating fibre length (L_A).

A comparison of the experimentally obtained torsional stroke parameters with the theoretical estimates are provided in Figure 16. The parameters used for calculating the theoretical values are given in Table 1.

Table 1. Measured parameters used in theoretical calculations of actuation stroke and torque for twisted nylon 6 fibre.

Temperature range	26 - 62ºC
Actuating fibre length (L_A)	70 mm
Free stroke per length (θ)	-2.45 º/mm
Initial torsional modulus of actuating fibre (k_A)	3.56×10^{-6} N.m^2
Final torsional modulus of actuating fibre (k'_A)	3.19×10^{-6} N.m^2
Torsional modulus of return spring fibre (k_N)	4.7×10^{-7} N.m^2

As seen for both the isotonic actuation tests (Figure 16(a)) and actuation tests against a return spring (Figure 16(b)), the agreement between measured and calculated values is very good. The close agreement indicates that the theoretical treatment based on torsion mechanics is a suitable method for evaluating torsional actuation in twisted fibres. In some cases, however, discrepancies were found between the measured and calculated values. The expected blocked torque determined from the parameters given in Table 1 of 136 μN.m was significantly less than the measured value of 225 μN.m. Similarly, the free stroke and torsional stiffness determined from the torque-stroke curve measured following the blocked torque measurement were higher than obtained directly from free stroke tests. The reasons for these discrepancies are not yet known, however, changes in the internal structure of the twisted fibre during the training cycles may be involved. Further studies are underway to investigate the effect of training on the structure and properties of the twisted fibres.

4. Conclusions

This paper has investigated test methods for characterising torsional actuators using a twisted oriented semicrystalline polymer fibre as the test subject and temperature change to induce actuation. An experimental method was designed and developed which was able to continuously measure thermally-induced torsional actuation of fibrous materials. Various different testing modes were studied that replicate possible application conditions: free stroke in a one-end-tethered fibre, torsional actuation against an externally applied torque (isotonic), blocked rotation to determine torque generated, and torsional actuation against a return spring fibre when operated in the two-end-tethered state. Theoretical prediction of torsional stroke generation of twisted fibre was developed using torsion mechanics that gave good agreement between experimental measurement and calculated values for the isotonic and return-spring experiments. The analysis allows the prediction of torsional stroke based on the fundamental characteristics of the actuator: free stroke and stiffness. Some discrepancy was noted in the estimation of the blocked torque. Further studies are underway to investigate whether 'training' cycles result in structural changes within the twisted fibres that may affect the torsional behaviour.

Acknowledgements

The authors thank the Australian Research Council for supporting this work through the Professorial Fellowship (GMS DP110101073), Centre of Excellence (CE 140100012) and Discovery Early Career Researcher Award (JF DE12010517). The authors also thank Mr Michael Tran for assistance in building the test apparatus; Mr Ali Jeirani (with financial support from the Australian National Fabrication Facility) for drawing Figure 2; and meaningful discussions with Professor Ray Baughman and his team at the University of Texas at Dallas and Professor John Madden (University of British Columbia).

References

[1] J. Foroughi, G.M. Spinks, G.G. Wallace, J. Oh, M.E. Kozlov, S. Fang, T. Mirfakhrai, J.D.W. Madden, M.K. Shin, S.J. Kim, R.H. Baughman, Torsional Carbon Nanotube Artificial Muscles, Science, 334 (2011) 494-497.

[2] M.D. Lima, N. Li, M. Jung de Andrade, S. Fang, J. Oh, G.M. Spinks, M.E. Kozlov, C.S. Haines, D. Suh, J. Foroughi, S.J. Kim, Y. Chen, T. Ware, M.K. Shin, L.D. Machado, A.F. Fonseca, J.D.W. Madden, W.E. Voit, D.S. Galvão, R.H. Baughman, Electrically, Chemically, and Photonically Powered Torsional and Tensile Actuation of Hybrid Carbon Nanotube Yarn Muscles, Science, 338 (2012) 928-932.

[3] K.-Y. Chun, S. Hyeong Kim, M. Kyoon Shin, C. Hoon Kwon, J. Park, Y. Tae Kim, G.M. Spinks, M.D. Lima, C.S. Haines, R.H. Baughman, S. Jeong Kim, Hybrid carbon nanotube yarn artificial muscle inspired by spider dragline silk, Nat Commun, 5 (2014).

[4] S.M. Mirvakili, A. Pazukha, W. Sikkema, C.W. Sinclair, G.M. Spinks, R.H. Baughman, J.D.W. Madden, Niobium Nanowire Yarns and their Application as Artificial Muscles, Advanced Functional Materials, 23 (2013) 4311-4316.

[5] W. Guo, C. Liu, F. Zhao, X. Sun, Z. Yang, T. Chen, X. Chen, L. Qiu, X. Hu, H. Peng, A Novel Electromechanical Actuation Mechanism of a Carbon Nanotube Fiber, Advanced Materials, 24 (2012) 5379-5384.

[6] C.S. Haines, M.D. Lima, N. Li, G.M. Spinks, J. Foroughi, J.D.W. Madden, S.H. Kim, S. Fang, M. Jung de Andrade, F. Göktepe, Ö. Göktepe, S.M. Mirvakili, S. Naficy, X. Lepró, J. Oh, M.E. Kozlov, S.J. Kim, X. Xu, B.J. Swedlove, G.G. Wallace, R.H. Baughman, Artificial Muscles from Fishing Line and Sewing Thread, Science, 343 (2014) 868-872.
[7] C.K. Andrew, P.C. Gregory, Thermo-mechanical characterization of shape memory alloy torque tube actuators, Smart Materials and Structures, 9 (2000) 665.
[8] K. Jaehwan, K. Byungwoo, Performance test and improvement of piezoelectric torsional actuators, Smart Materials and Structures, 10 (2001) 750.
[9] R.K. Josephson, Contraction Dynamics and Power Output of Skeletal Muscle, Annual Review of Physiology, 55 (1993) 527-546.
[10] J.D.W. Madden, N.A. Vandesteeg, P.A. Anquetil, P.G.A. Madden, A. Takshi, R.Z. Pytel, S.R. Lafontaine, P.A. Wieringa, I.W. Hunter, Artificial muscle technology: physical principles and naval prospects, Oceanic Engineering, IEEE Journal of, 29 (2004) 706-728.
[11] J.E. McIntyre, Synthetic Fibres: Nylon, Polyester, Acrylic, Polyolefin, Elsevier Science2004.
[12] O. Olabisi, K. Adewale, Handbook of Thermoplastics, Taylor & Francis1997.
[13] P. Mitchell, G.R.S. Naylor, D.G. Phillips, Torque in Worsted Wool Yarns, Textile Research Journal, 76 (2006) 169-180.
[14] A.D. McNaught, A. Wilkinson, I.U.o. Pure, A. Chemistry, Compendium of Chemical Terminology: IUPAC Recommendations, Blackwell Science1997.
[15] T. Shibukawa, V.D. Gupta, R. Turner, J.H. Dillon, A.V. Tobolsky, Temperature Dependence of Shear Modulus and Density of Nylon-6, Textile Research Journal, 32 (1962) 1011-1012.

Figure 1. a) Illustration of different torsional actuation methods where the actuating element is optionally subjected to an external torque (presented as force applied by a hanging weight) and / or a return spring fibre; **b)** theoretical estimates of torsional stroke at each point along the length of an actuating fibre and return spring (non-actuating) fibre, if used, and operated in free rotation or isotonic rotation modes.

Figure 2. Schematic illustration of twist insertion in Nylon 6 (graphics are not to scale).

Figure 3. CAD model of torsional actuation test apparatus; (1) heating zone, (2) ultra-low friction air bearing, (3) lever arm force/distance transducer, (4) movable fibre gripping clamp, (5) support for air bearing, (6) connecting fibre between lever arm force/distance transducer and bearing shaft, (7) actuating muscle fibre, and (8) fibre acting as return spring keeping the actuating muscle straight and well positioned.

Figure 4. Torsional actuation testing set-up; (1) test apparatus, (2) lever arm force/distance transducer, (3) lever arm controller, (4) DC power supply, (5) programmable temperature controller.

Figure 5. Optical micrographs of (a) precursor nylon 6 fibre, (b) twisted fibre with twist-induced coil section, (c) extracted twisted section, and (d) observed bias angle from higher magnification micrograph of twisted section. The diagonal markings observed in (c) and (d) arise from extrusion marks originally oriented along the axis of the untwisted fibre.

Figure 6. Torsional properties of twisted fibre prepared from 550 μm diameter nylon 6 and tested at room temperature: (a) shaft rotation against mechanical torque, and (b) torsional stiffness of different lengths of fibre with the slope giving the torsional modulus.

Figure 7. Torsional properties of nylon 6 fibres (a) shaft rotation against mechanical torque of different diameter fibre, and (b) torsional stiffness with resultant modulus.

Figure 8. Fibre rotation at 60ºC against applied mechanical torque. The inverse slope of the rotation/torque curve defines the torsional stiffness.

Figure 9. Optically measured torsional actuation of twisted nylon 6 during slow heating and cooling. The 70 mm long, 550 μm diameter fibre was attached to air bearings that allowed one end of the fibre to rotate freely with negligible friction. Negative values of torsional stroke represent untwisting. Arrows indicate the heating and cooling directions.

Figure 10. Isotonic constant torque (68 μN.m) actuation stroke of twisted nylon 6 over 6 consecutive heat/cool cycles.

Figure 11. Cycle based constant torque actuation profile of twisted nylon 6. Mechanical torque at the levels indicated was increased step-by-step corresponding to successive actuation cycles. A final heat/cool cycle was also performed at the original torque value (denoted RE for repeat).

Figure 12. Thermally-induced torque generation by twisted nylon 6 after free rotating training cycles.

Figure 13. Torque-stroke curves of nylon 6 fibre; (a) isometric force generation followed by free rotation on torque relaxation/regeneration, and (b) torque vs torsional stroke; trend extracted from isothermal section.

Figure 14. Variable torque actuation profile of Nylon 6 with multi-cycle test validation.

Figure 15. (a) Actuation profile of twisted Nylon 6 fibre during heating and cooling and operated with different return spring lengths. A small constant torque of 68 μN.m was also applied by the lever arm measurement system. Tests were performed with progressively shorter return spring lengths and a final repeat test using the original return spring length (denoted RE for repeat). (b) Final torsional stroke at 60^{o}C (untwisting) and when cooled to 26^{o}C (retwisting) at different return spring lengths.

Figure 16. Comparison of experimentally measured and theoretically calculated torsional strokes (equation 7) for 70mm long twisted nylon 6 fibre: (a) isotonic torsional stroke when operated against a constant external torque; (b) torsional stroke when using return springs of different lengths.

Figure 1:

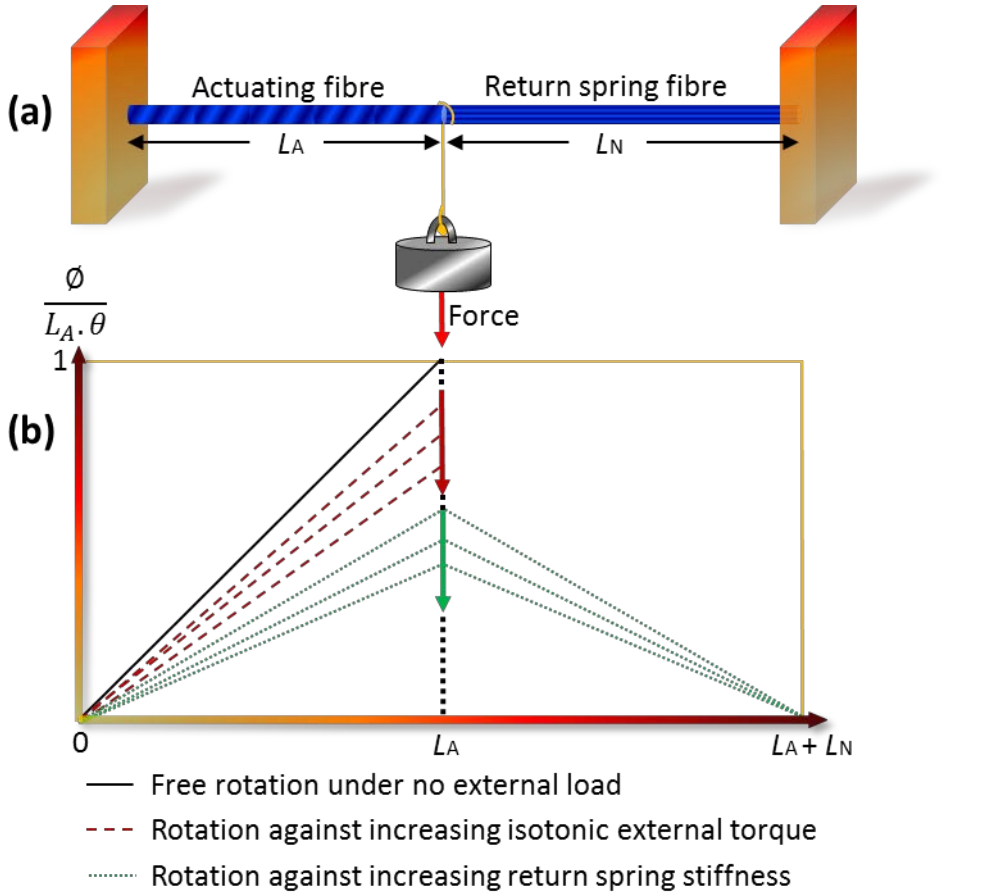

Figure 2:

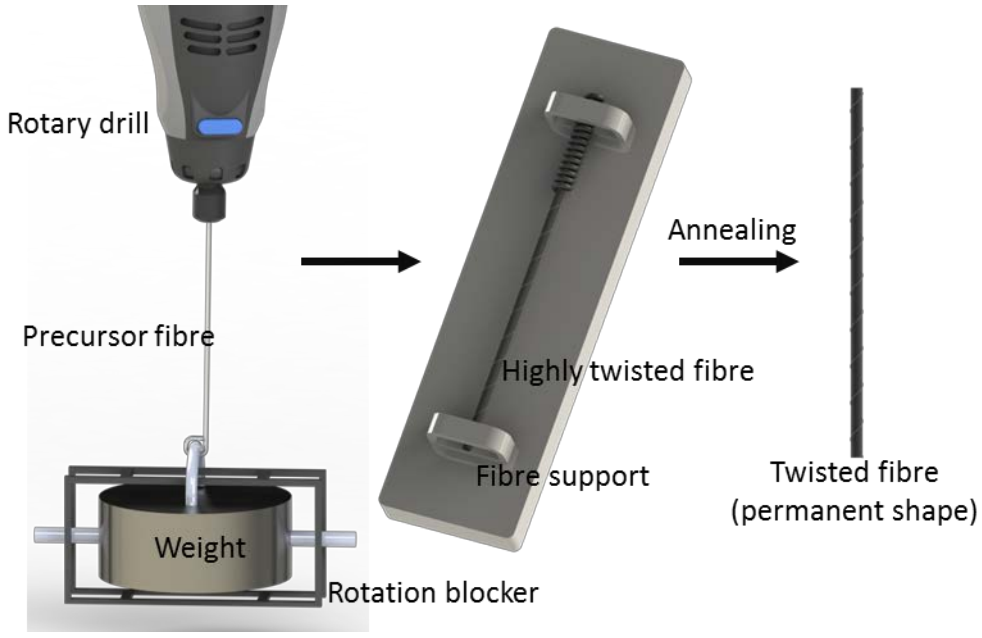

Figure 3:

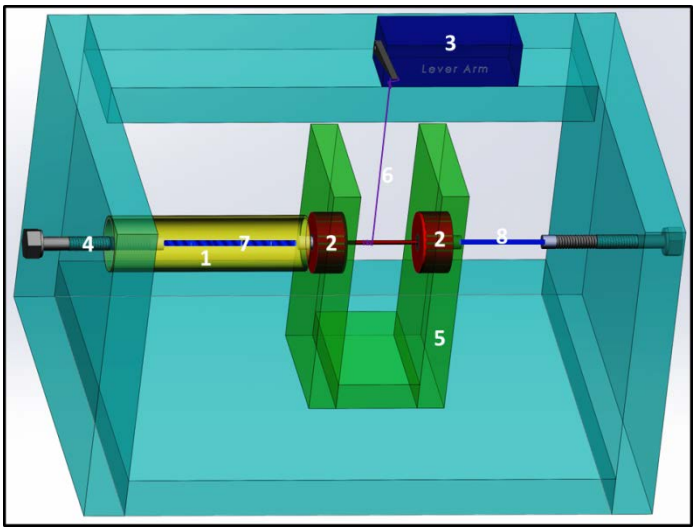

Figure 4:

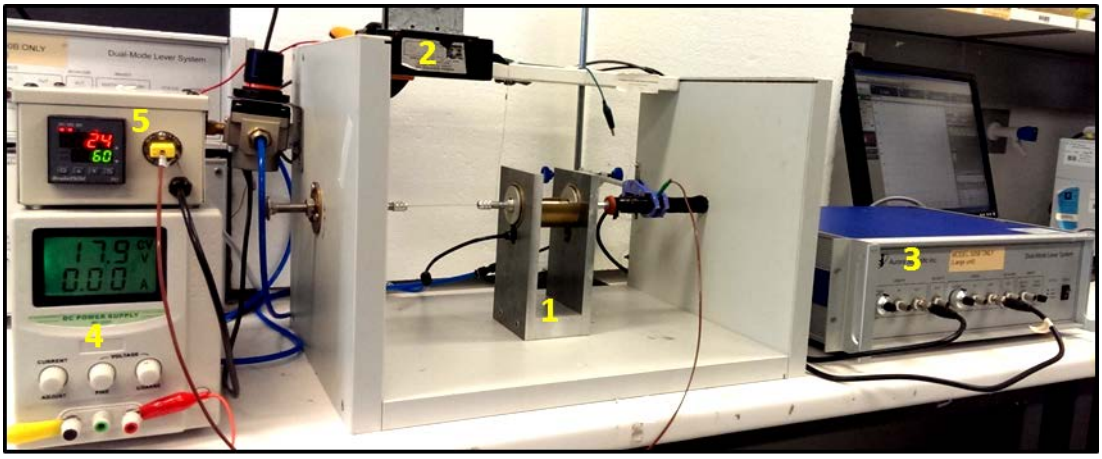

Figure 5:

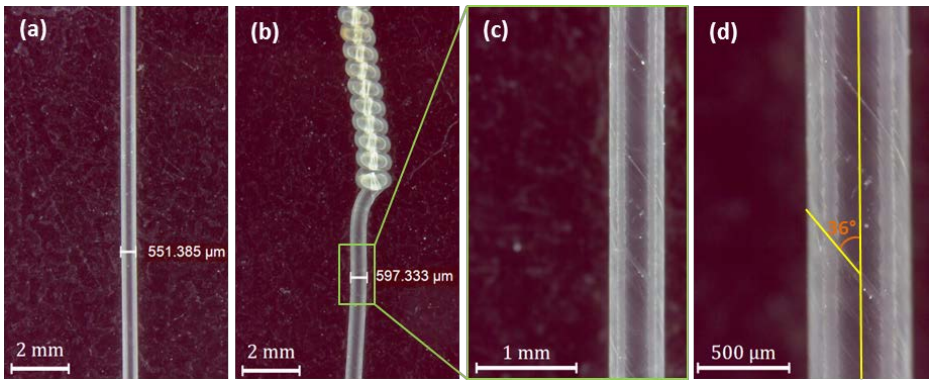

Figure 6:

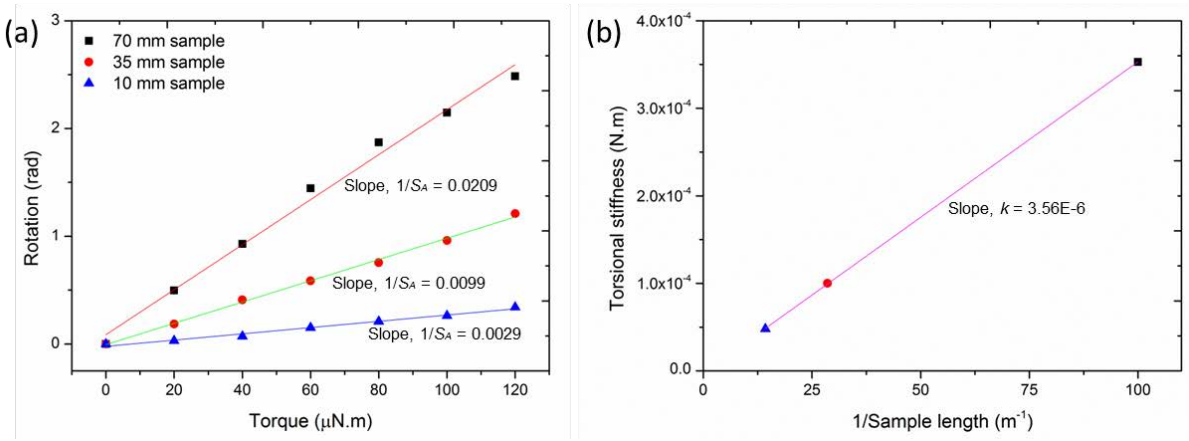

Figure 7:

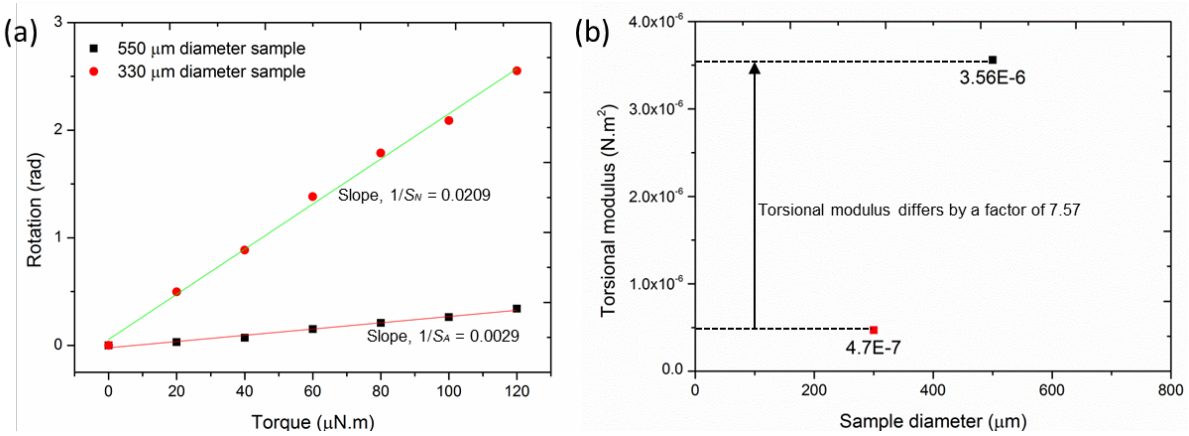

Figure 8:

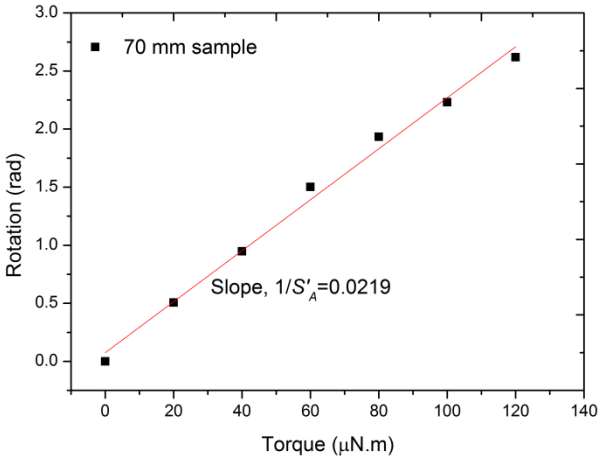

Figure 9:

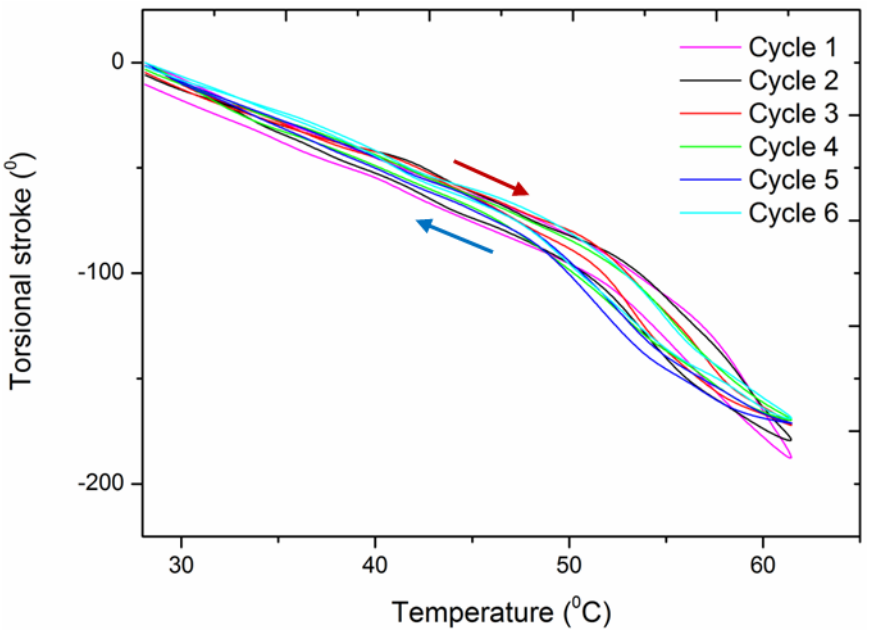

Figure 10:

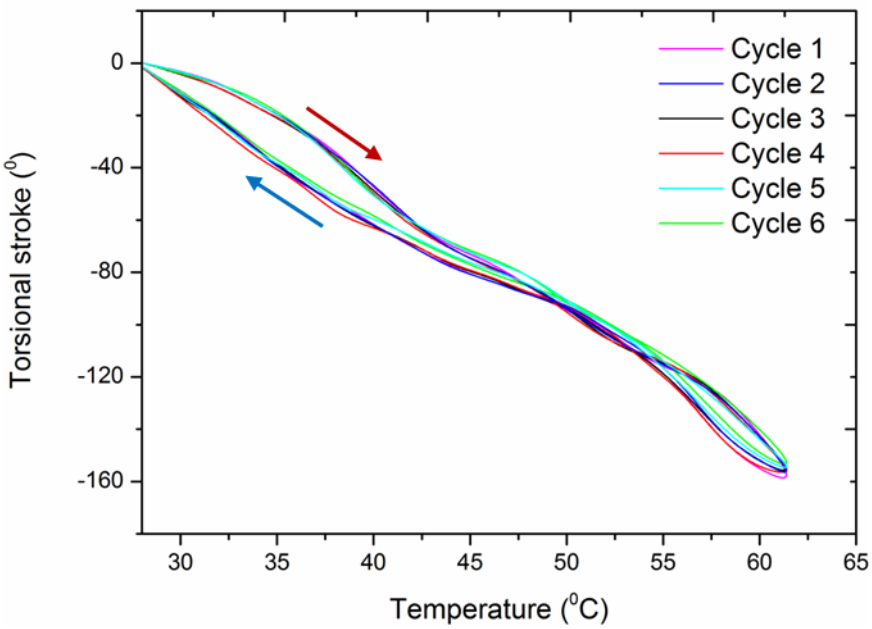

Figure 11:

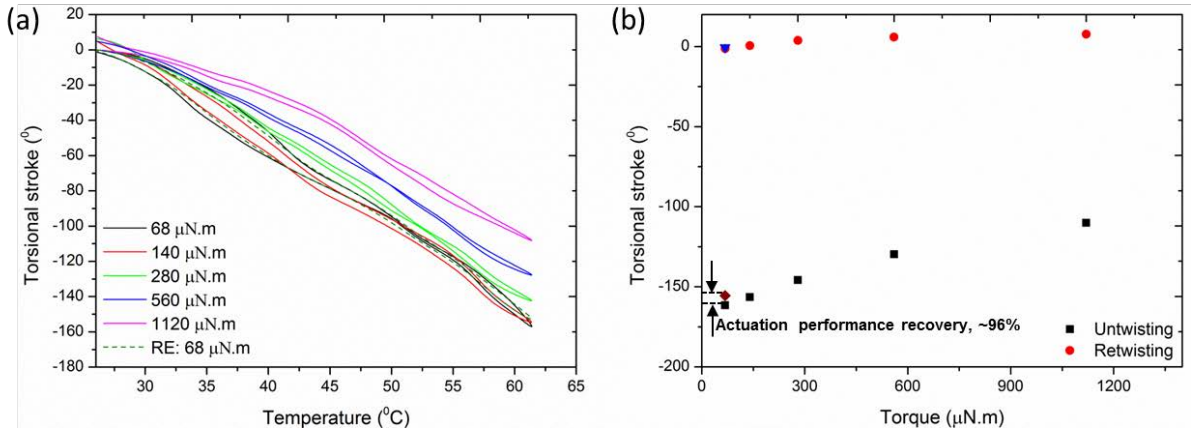

Figure 12:

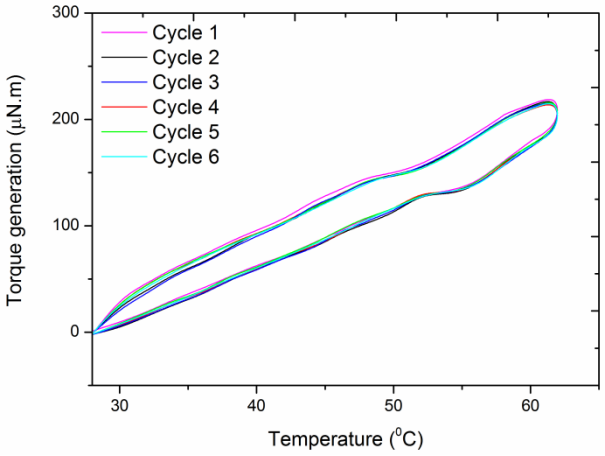

Figure 13:

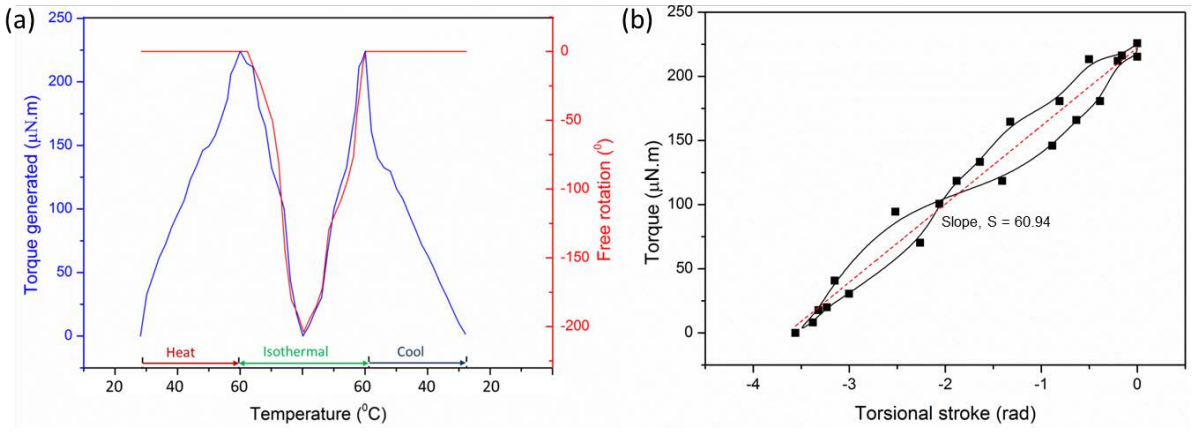

Figure 14:

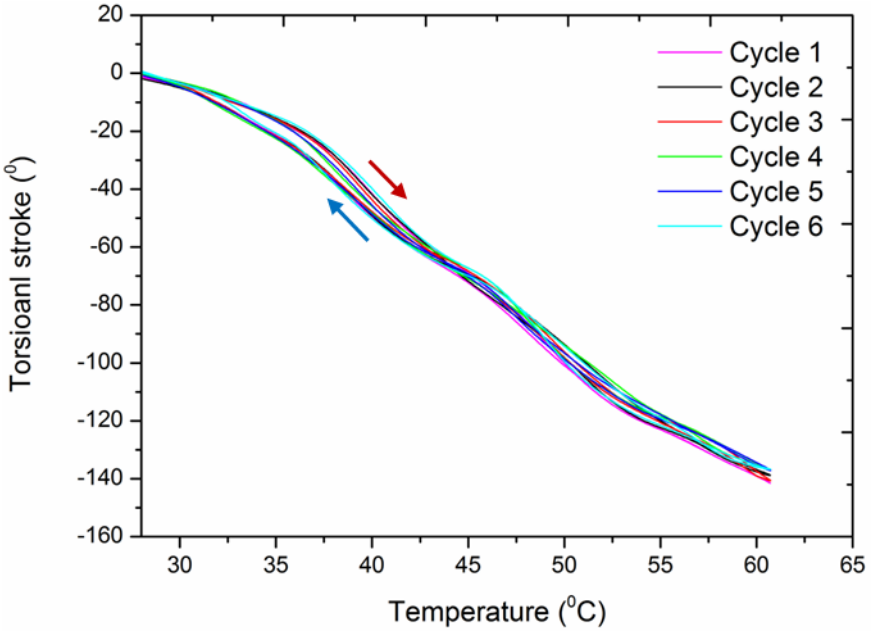

Figure 15:

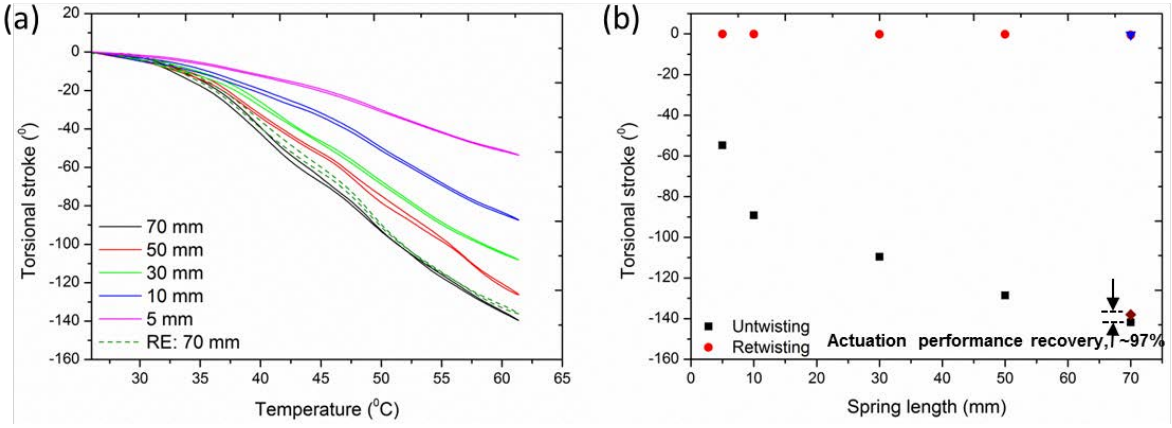

Figure 16:

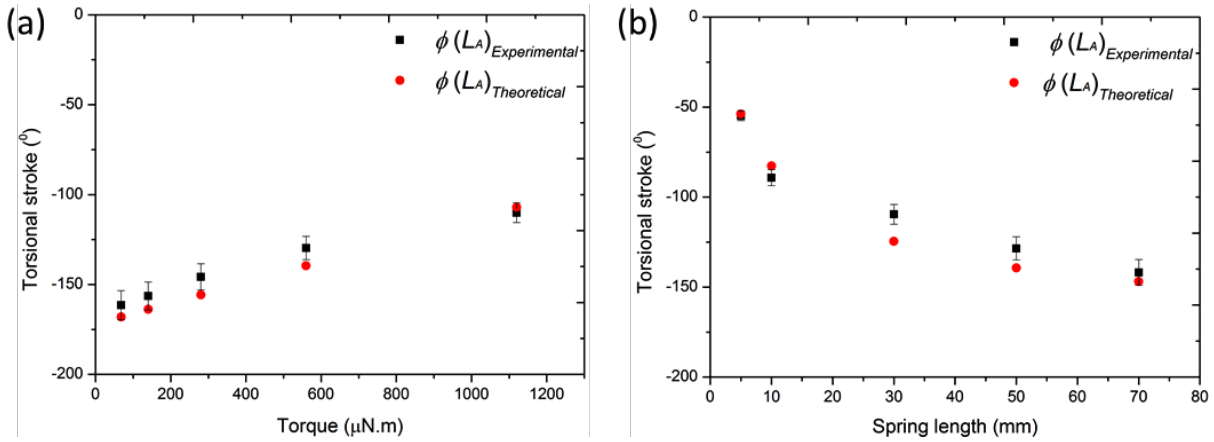
(a)
Torsional stroke (°)
Torque (μN.m)
$\phi(L_A)_{Experimental}$
$\phi(L_A)_{Theoretical}$
(b)
Torsional stroke (°)
Spring length (mm)
$\phi(L_A)_{Experimental}$
$\phi(L_A)_{Theoretical}$